JOURNAL OF BACTERIOLOGY, Sept. 1979, p. 961-976
0021-9193/79/09-0961/16$02.00/0

Vol. 139, No. 3

Specificity in Formation of Type II F′ Plasmids

R. G. HADLEY AND RICHARD C. DEONIER*

Molecular Biology, University of Southern California, University Park, Los Angeles, California 90007

Received for publication 26 June 1979

Eight new F′ plasmids derived from Hfr strains in which F is integrated at the chromosomal element $\alpha_3\beta_3$ have been isolated and subjected to restriction enzyme, hybridization, and electron microscope heteroduplex analysis. Plasmids carrying extensive amounts of bacterial deoxyribonucleic acid were produced even though they were obtained by selection for transfer of *lac*, which is closely linked to F in the parental Hfr strains. Seven plasmids were type II F*lac*$^+$ *proC*$^+$ *purE*$^+$ plasmids, and one was a type I F*lac*$^+$ *proC*$^+$ plasmid. Five of the F*lac*$^+$ *proC*$^+$ *purE*$^+$ plasmids contain approximately 284 kilobases of bacterial deoxyribonucleic acid, which is identical for all five within the resolution of the restriction enzyme analysis. These results indicate that type II F′ plasmids are the predominant *tra*$^+$ F′ type from this region of the *Escherichia coli* K-12 chromosome and that the recombination events leading to formation of these plasmids exhibit site specificity.

F′ plasmids carrying various bacterial genes have been known for nearly two decades (for reviews, see references 32 and 43). Scaife placed F′ plasmids into two categories: type I plasmids, which carry bacterial genes from only one side of the integrated F sequences in an Hfr, and type II plasmids, which carry genetic markers from both sides of the integrated F. F′ plasmids containing varied lengths of bacterial DNA can be formed from a single Hfr strain (28), and in some cases, genetically indistinguishable F′ plasmids arise independently from the same Hfr strain (4). Both type I and type II F′ plasmids have been analyzed by electron microscope heteroduplex methods (see, for example, references 26 and 44), and these studies have identified sites on F that can serve as recombinational "hot spots" that are active in F integration and in type I F′ excision (14). In most cases these are the transposable elements IS*2*, IS*3*, or $\gamma\delta$. The nature of recombination sites on the bacterial chromosome that may act during type I or type II F′ excision is still poorly defined.

One type of F′ plasmid that has been obtained repeatedly from two different types of Hfr strains is the F*lac*$^+$ *proC*$^+$ *purE*$^+$ (4, 7, 23, 28). The repeated formation of this F′ type could result from sites on the bacterial DNA that are hot spots for F′ excision. In this study, we describe the localization of excision sites leading to formation of a new set of F*lac*$^+$ *proC*$^+$ *purE*$^+$ plasmids from several Hfr strains whose points of origin are identical to those of Hfr strains P804 and OR11, the progenitors of other F*lac*$^+$ *proC*$^+$ *purE*$^+$ plasmids (4, 28). Unlike the plasmids obtained by Berg and Curtiss (4), the plasmids described here were obtained by selection for transfer of the *lac* operon, which is closely linked to the integrated F in these Hfr strains. With this selection, there should not have been a predisposition toward large F′ plasmids. Seven of the eight plasmids physically characterized in this study are shown to be type II, which contrasts with interpretations from previous data from a variety of chromosomal regions (32). We have localized the excisional recombination sites on the bacterial DNA to a limited set of fragments arising from digestion with *Eco*RI, and we conclude that there is site specificity in the excision process.

In addition, the data provide new information on the role of the bacterial IS*3* element $\alpha_3\beta_3$ as an integration site for F, and the presence of a modified form of the F plasmid having an additional IS*3* element is documented.

MATERIALS AND METHODS

Strains. Strains used for isolation, testing, and maintenance of F′ plasmids are described in Table 1. The Hfr strains used were those derived by Curtiss from the K-12-112 subline or the W1485 subline of *Escherichia coli* K-12 (4, 13), or were constructed by Broda from the W1655 derivative of W6F$^+$ (6). The approximate points of origin and transfer orientations were verified by cross-streak matings with AB1157 or χ478 recipient strains.

Isolation of F′ strains. Secondary F′ strains used for physical analysis were obtained by mating Hfr strains with the *recA56* recipient RH63 and selecting for Lac$^+$ Str^r transconjugants. Mating protocols employed transfer from patches of Hfr clones to recipi-

TABLE 1. *Bacterial strains and plasmids*

Strain	Genotype	Source/reference
Hfr		
χ435(OR6)	Prototroph	4, 13
χ493(OR11)	Prototroph	4, 13
χ892(OR72)	Prototroph	4, 13
ED942(B5)	*metB1 rel-1* λ^r	6
F		
AB1157	*thi-1 argE3 his-4 proA2 leu-6 thr-1 lacY1 galK2 ara-14 mtl-1 xyl-5 rpsL31 tsx-33 sup-37*	21
AB2463	*thr-1 leu-6 thi-1 argE3 his-4 proA2 lacY1 galK2 mtl-1 xyl-5 ara-14 tsx-33* λ*-supE44 rpsL31 recA13*	25
χ478	*ara leu T1^r lacZ proC tsx purE trp lys rpsL mtl xyl metE thi*	13
PB314	*lac purE thi tsx rpsL*	7
ED1111	*lac purE thi tsx rpsL recA*	8
RD17	*thi-1, rel-1,* Δ*(proB-lac)*$_{X111}$ *supE44 recA56*	19
RH63	RD17 Str^r	Spontaneous mutant of RD17
F′		
RH1	ED1111(pRH1); pRH1 = F *lac*$^+$ *proC*$^+$ *purE*$^+$	Hfr OR6 × RH63 (selection: Lac$^+$ [Str^r]^a); conjugational transfer to ED1111
RH7	ED1111(pRH7); pRH7 = F *lac*$^+$ *proC*$^+$ *purE*$^+$	Hfr OR11 × RH63 (selection: Lac$^+$ [Str^r]); conjugational transfer to ED1111
RH17	ED1111(pRH17); pRH17 = F *lac*$^+$ *proC*$^+$ *purE*$^+$	Hfr OR72 × RH63 (selection: Lac$^+$ [Str^r]); conjugational transfer to ED1111
RH38	ED1111(pRH38); pRH38 = F *lac*$^+$ *proC*$^+$ *purE*$^+$	Hfr B5 × RH63 (selection: Lac$^+$ [Str^r]); conjugational transfer to ED1111
RH95, RH97, RH98	Prototrophs; primary F *lac*$^+$ *proC*$^+$ *purE*$^+$	Fluctuation enrichment from OR11
RH96	Prototroph; primary F *lac*$^+$ *proC*$^+$	Fluctuation enrichment from OR11
AT3155	Δ*lac-175*(i$^-$) *rpsL*/F42-1 *lacI78*(i^c)	26
RD22	*thi-1 rel-1* Δ*(proB-lac)*$_{X111}$ *supE44 recA56*/ ORF203	19
RH111	AB2463(pRH111); pRH111 = *tra*Δ F*proA*$^+$	Hfr OR6 × AB2463 (selection: pro$^+$ [Str^r])
F$^+$		
W1485	*thi*/F$^+$	44
W1655	*metB1 rel-1* λ^r/FΔ(33-43)	2

[a] Discriminating character used for donor contraselection.

ents by replica plate techniques (i.e., with no interruption). Primary F′ strains were obtained by fluctuation enrichment procedures (6), with enrichment continued on sample cultures showing elevated *lac* transmission to ED1111. The presence of Tra$^+$ F*lac*$^+$ *proC*$^+$ *purE*$^+$ plasmids was confirmed by the formation of *lac*$^+$ and *purE*$^+$ transconjugants in matings with the *recA* recipient ED1111, by transfer of *proC*$^+$ to χ478, and by examination of plasmid DNA. F′ isolates were stored at −20°C in 40% glycerol and 50% L-broth immediately after marker analysis.

Media. Minimal medium (12) was supplemented to 20 μg/ml with amino acids, to 0.2% with the appropriate sugar, to 20 μg/ml with deoxyadenosine, and to 1 μg/ml with thiamine. L-broth or L-agar (31) was used for matings and for purification or growth for routine genetic testing. Tryptone broth contained 10 g of tryptone per liter, 5 g of NaCl per liter, 1 μg of thiamine per ml, and 0.2% glucose (pH 7.4). MacConkey agar (Difco) was employed in screening for Lac colonies. Eosin methylene blue agar (Difco) supplemented with glucose to 0.2% was used for tests of sensitivity to the male-specific bacteriophage f2 by the cross-streak method. For preparation of the F*lac*$^+$ *proC*$^+$ *purE*$^+$ plasmid DNA, strains with the ED1111 genetic background were cultured in minimal media containing lactose and thiamine, thus selecting simultaneously for retention of the *lac*$^+$ and the *purE*$^+$ characters.

Isolation of DNA. Plasmid DNA was prepared by the methods of Bazaral and Helinski (3) and Sharp et al. (44). Fifty milliliters of spheroplast-forming solution (1 mg of lysozyme per ml, 0.1 mg of RNase per ml, and 0.1 g of sucrose per ml) in TES (0.05 M Tris, 0.05 M NaCl, 0.005 M EDTA, pH 8.5) was used to resuspend washed bacterial pellets containing approximately 10^{12} bacteria. Recent experiments indicated that concentrations of lysozyme, sucrose, and RNase could be reduced by half to provide equivalent or slightly improved final yields of plasmid DNA. After incubation of the resuspended cells at 37°C for 10 min,

lysis was achieved by adding 25 ml of 2% sodium lauroyl sarcosine in TES. Incubation at 37°C was continued for 10 min with frequent stirring. The lysate was drawn back and forth a minimum of 14 times through a 5-ml plastic pipette (Falcon) at 1 to 2 ml/s to shear the chromosomal DNA. Lysates were adjusted to a density of 1.51 g/ml and 250 μg of ethidium bromide per ml by addition of 0.86 g of CsCl and 0.03 g of ethidium bromide solution (10 mg/ml in TES) per g of lysate. Samples were centrifuged as previously described (19). Ethidium bromide was removed from DNA samples by isoamyl alcohol extraction, followed by dialysis against a cation exchange resin (44). DNA was stored in 0.01 M Tris–0.01 M NaCl–0.001 M EDTA (pH 8.0) at 4°C (11).

Restriction endonuclease digestion. Restriction endonuclease *Eco*RI was obtained from Miles Laboratories. Reaction conditions of Morrow et al. (36) were employed, and digestion was usually with a 1.5- to 3.0-fold enzyme excess. Reactions were quenched by chilling reaction mixtures on ice and adding EDTA to approximately 10 mM. Samples were then dialyzed against a 1:20 dilution of electrophoresis buffer (48). Restriction endonuclease *Bam*HI was also obtained from Miles Laboratories, and the reaction conditions specified by the source were employed.

Agarose gel electrophoresis. Samples (0.05 ml) in a 1:20 dilution of electrophoresis buffer were evaporated to dryness with a jet of dry air and suspended in 10 μl of distilled water containing 25% sucrose. Slab gels (140 mm long, 3 mm thick, and containing 0.7% agarose) were run at 2.3 V/cm for 3 to 7 h, and tube gels (220 mm long and containing 0.7% agarose) were run at 1.4 V/cm for 24 to 36 h with periodic buffer changes. Mobility standards were *Eco*RI fragments of lambda (λcI857*S*7) DNA (47) and F DNA (10), with F fragment sizes adjusted to correspond to a molecular size of 94.5 kilobases (kb), which facilitates comparison with previous mapping data. For high-resolution experiments (tube gel conditions), most samples and molecular weight standards were run in triplicate. The relative mobility values showed standard deviations of 0.2%. Gels were stained in 50% electrophoresis buffer containing 0.5 μg of ethidium bromide per ml for 30 min and were destained with three to four rinses of deionized water over a 5- to 10-min interval. Gels were transilluminated with long-wave UV light and were photographed using either Kodak Plus X or Polaroid 55 P/N films and Kodak red (no. 23A) and yellow (no. 9) filters in combination.

Mobility analysis. Photographic negatives were scanned with a Joyce-Loebl microdensitometer. Calibration curves based upon F and λ *Eco*RI fragments were constructed by plotting the logarithm of the molecular size in kb as a function of fragment mobility relative to fragment f3 of F. For high-resolution experiments, relative mobility for the largest molecular size values was expressed as a quadratic function of the logarithm of the molecular size by using a least-squares curve-fitting process. This allowed greater precision in assignment of molecular sizes to fragments. For the few remaining multiple bands that were unresolved, the number of fragments per band was determined by comparing the areas of the densitometer peaks of the multiple band to the areas of adjacent single bands. Peak areas were determined by using a Numonics Graphics Calculator.

Hybridization techniques. DNA from agarose gels was transferred to nitrocellulose filters by the method of Southern (45) as modified by Engel and Dodgson (22). Hybridization probes were *Eco*RI fragments f2 and f4 of F cloned on RSF2124 (1; Deonier and Hadley, manuscript in preparation). Fragments of f2 and f4 DNA were purified from vehicle DNA by sedimentation through a sucrose gradient. These probes were labeled by the nick translation method (42) to specific activities of 5×10^6 to 5×10^7 cpm/μg using ^{3}H-labeled dTTP at 90 Ci/mmol and ^{3}H-labeled dATP, dCTP, and dGTP at 20 Ci/mmol (ICN Pharmaceuticals, Inc.). The labeled f2 or f4 probes were hybridized to the DNA on the filters for 40 to 90 h at 65°C in a solution consisting of 10× Denhardt solution (16) in 3 × SSC (1× SSC is 0.15 M NaCl plus 0.015 M sodium citrate, pH 7.0), 50 μg of salmon sperm DNA per ml, and 0.1% SDS. Fluorography of the filters was performed at −70°C with Kodak XR-5 X-ray film preflashed to 0.2 to 0.4 absorbance units (30) for 20 to 200 h.

Electron microscopy. Samples were mounted for electron microscopy by using the formamide technique as previously described (15, 17). Molecules were examined with a JEM7 electron microscope, and projected images from micrographs were measured by using a Numonics Graphics Calculator. The size reference standard was FΔ(33–43) (taken to be 83.8 kb), with φX174 taken as the intermediate size standard.

RESULTS

The plasmids examined in this study are very large. As an aid to understanding the data to be presented, a summary of the conclusions is provided in Fig. 1. The eight F′ plasmids pRH1, pRH7, pRH17, pRH38, pRH95, pRH96, pRH97, and pRH98 were obtained from the four indicated Hfr strains. All plasmids except pRH96 extended beyond *lac* to include *purE*, and all plasmids except pRH96 are type II (i.e., they include bacterial DNA from both sides of the integrated F in the Hfr strains). The junctions between F DNA and bacterial DNA were identified by mobility analysis, by hybridization, and by electron microscope heteroduplex procedures.

Analysis of bacterial *Eco*RI restriction fragments carried by the seven type II F′ plasmids reveals that the counterclockwise excision endpoint lies within the same *Eco*RI restriction fragment in all cases. In five of the cases (pRH1, pRH7, pRH95, pRH97, and pRH98), the clockwise endpoints also lie within a single bacterial *Eco*RI restriction fragment, and they contain identical bacterial DNA segments even though they represent independent isolates from two different Hfr strains. The clockwise endpoints of pRH38 and pRH17 differ from the endpoint shared by the other five.

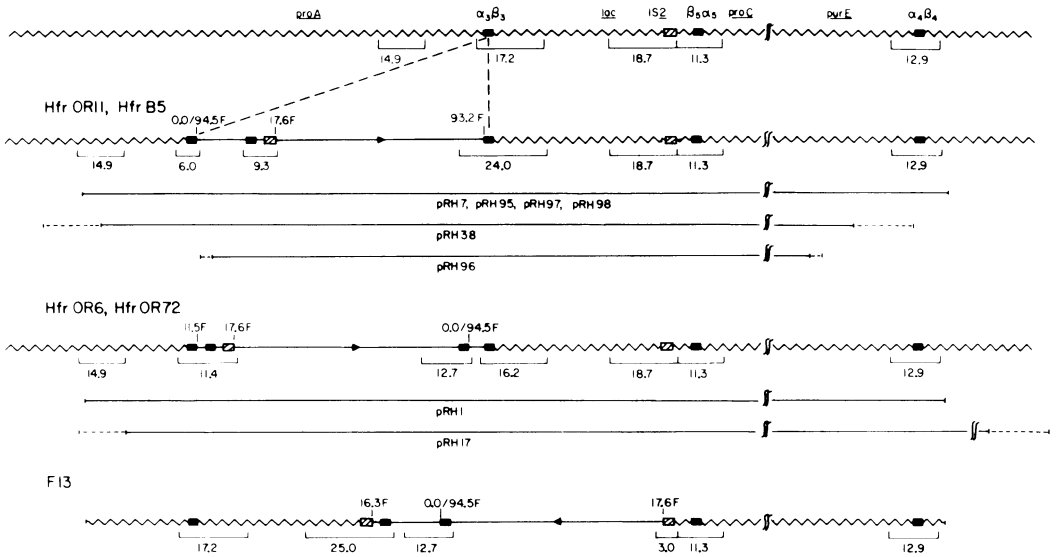

FIG. 1. *Summary of the physical structures of the F′ plasmids examined in this work. A physical map of a portion of the bacterial chromosome and the approximate locations of selected genes and IS elements are shown at the top of the figure. A portion of the bacterial DNA between proC and purE has been omitted for clarity. (For distances between IS elements, see Fig. 1 in ref. 26.) Below this, the sequence arrangement of the Hfr strains OR11 and B5 is compared with the sequence arrangement of the Hfr strains OR6 and OR72. The physical structure of the F′ F13 (26) is shown at the bottom of the figure. Sawtooth lines represent bacterial DNA, and smooth lines represent the integrated F sequences. Selected F coordinates are indicated (14). Various IS3 elements (with their corresponding names in the αβ notation) are indicated by solid boxes, and IS2 elements are designated by hatched boxes. The locations of EcoRI fragments containing IS2 or IS3 elements, junctions between F and bacterial DNA, or other relevant DNA segments are indicated by brackets, and the fragment sizes are shown (cf. Table 3). Span lines below the Hfr maps indicate the extent of the DNA contained on the F′ strains derived from these Hfr strains. Dashed termini for some span lines indicate the resolution of the endpoint determination. Exact correspondence of the pRH1, pRH7, pRH95, pRH97, and pRH98 termini with those of F13 is indicated, based on the exact correspondence of EcoRI fragments derived from the termination regions of these five plasmids and of F13. The clockwise termini for pRH1, pRH7, pRH95, pRH97, and pRH98 all fall within the first EcoRI fragment clockwise of f($\alpha_4\beta_4$), the fragment containing $\alpha_4\beta_4$. This conclusion is based on the following reasoning. All of the bacterial EcoRI restriction fragments that lie completely between $\alpha_3\beta_3$ and $\alpha_4\beta_4$ (defined largedly by ORF203), as well as all of the bacterial EcoRI fragments lying between the 14.9-kb fragment and f($\alpha_3\beta_3$) (Table 4), are generated from these plasmids. The only EcoRI fragment not accounted for by these bacterial fragments corresponds to the novel joint. Because complete EcoRI fragments clockwise of f($\alpha_4\beta_4$) do not appear in these plasmids, it is concluded that the clockwise excision termini lie in the EcoRI fragment immediately clockwise of f($\alpha_4\beta_4$).*

The sequence organization of the integrated F in Hfr strains OR6 and OR72 indicates that these strains were formed by integration of an altered F plasmid at an additional copy of IS*3* not normally found in the F plasmid. This additional IS*3* is located at 11.5 F on the standard F map.

Isolation and genetic analysis of F′ plasmids. F′ plasmids were identified by their ability to transfer *lac* to appropriate recipients. Preliminary analysis indicated that the major F′ class obtained from each of the four Hfr strains carried genetic markers clockwise but not counterclockwise of the Hfr point of origin. Of 19 such F′ plasmids, 18 contained *purE*$^+$ in addition to *lac*$^+$, whereas one (pRH96) was an F*lac*$^+$ *proC*$^+$ plasmid. No plasmids like the classical F*lac* (F42) were obtained. Seven of the 18 strains were further characterized and were found to be capable of transferring *proC*$^+$ to χ478, indicating that they contained F*lac*$^+$ *proC*$^+$ *purE*$^+$ plasmids. Genetically identical plasmids had been previously isolated from OR11 by Berg and Curtiss (4), who selected for transmission of *proC*$^+$ rather than *lac*$^+$. In the present experiments, the F*lac*$^+$ *proC*$^+$ *purE*$^+$ class of plasmids was obtained both by replica plate matings (pRH1, pRH7, pRH17, and pRH38) (no interruption) and by fluctuation enrichment procedures (pRH95, pRH97, and pRH98), indicating that the production of this type of F′ plasmid is determined by excisional processes in the donor Hfr strains. Since this class was obtained from Hfr strains belonging to the W1485, K-12-112,

and W6 sublines, these excisional processes apparently are a common feature of *E. coli* K-12 strains.

The eight plasmids listed above, which contain a portion of the bacterial chromosome that has previously been subjected to extensive electron microscope heteroduplex mapping (20, 26), were analyzed physically to determine their sequence arrangement and to locate their excision endpoints. All plasmids were analyzed by restriction enzyme techniques (48), and four of the seven F*lac*$^+$ *proC*$^+$ *purE*$^+$ plasmids (pRH1 from Hfr OR6, pRH7 from Hfr OR11, pRH17 from Hfr OR72, and pRH38 from Hfr B5) were analyzed more extensively by both electron microscope heteroduplex procedures and hybridization methods.

Molecular length determination. Molecular lengths were determined by electron microscopy or by restriction analysis (Table 2). No molecular length heterogeneity was detected in any of the samples by either technique. The sizes of all F' plasmids are consistent with the sizes indicated by genetic analysis. It is seen that the molecular lengths of pRH1, pRH7, pRH95, pRH97, and pRH98 are identical within experimental error. It will be shown below that these plasmids carry bacterial sequences that are identical to the extent that can be determined by the methods employed here. The pRH38 plasmid is definitely shorter than all others except pRH96, and by more than can be accounted for by its Δ(33-43) deletion alone. This deletion is present because the FΔ(33-43) plasmid from which the parental Hfr strain B5 arose was correspondingly deleted (2). The largest plasmid, pRH17, is large enough to carry as much as 9% of the bacterial chromosome. As expected, pRH96, the F*lac*$^+$ *proC*$^+$, is the smallest of the set.

TABLE 2. *Molecular lengths of Flac*$^+$ *proC*$^+$ *purE*$^+$ *plasmids from E. coli K-12*

Plasmid	Molecular length (kb)		Reference
	Electron microscopic	Electrophoretic[a]	
pRH1	373 ± 11	379 ± 3	This research
pRH7	376 ± 14	379 ± 3	This research
pRH38[b]	362 ± 9	356 ± 3	This research
pRH17	473 ± 16	484 ± 3	This research
pRH96	—[c]	297	This research
pRH97	—	>374[d]	This research
ORF203	334 ± 11	335 ± 3	20; This research
F13	385 ± 6	—	26

[a] Restriction fragments smaller than 0.7 kb to 0.5 kb not included.

[b] The F sequences of this plasmid have a 10-kb deletion (2).

[c] —, Not determined by this method.

[d] Smallest bands were not analyzed. Estimated upper bound is no more than 5 kb larger than the size given. Plasmids pRH95 and pRH98 showed identical restriction enzyme digest products, and it is therefore concluded that they have the same molecular length as pRH97.

Linkage between bacterial and F sequences in pRH1, pRH7, pRH17, and pRH38. (i) General analysis. The integration site of F can be localized within a specific F *Eco*RI fragment from principles outlined in Fig. 2 (5). Consider the IS*3*, $\alpha_1\beta_1$, located in *Eco*RI fragment f2 of F. When integration occurs at $\alpha_1\beta_1$, fragment f2 will be separated into two junction fragments (f2A and f2B), each of which will be joined to bacterial sequences as part of a new restriction fragment. If the integration occurs at an IS*3* on the bacterial chromosome, each of the new fragments will contain an IS*3* element located at the junction of F and bacterial DNA. Because *Eco*RI fragment f4 of F will not be altered by recombination in this case, fragment f4 will migrate with its usual mobility. If integration were to occur at $\alpha_2\beta_2$ on F (i.e.,

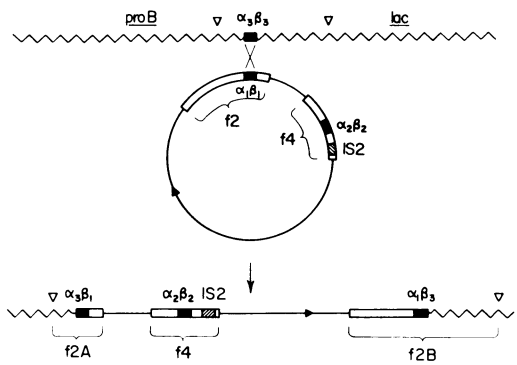

FIG. 2. *Alterations in the physical linkage of F DNA resulting from F integration within EcoRI fragment f2 at the bacterial IS3* $\alpha_3\beta_3$. *Structural designations are the same as in Fig. 1. The open-boxed regions represent EcoRI fragments f2 and f4 of F. Relevant EcoRI cleavage sites on F are the ends of f2 and f4, and the EcoRI sites of interest on the bacterial DNA appear as open triangles. DNA originally present in f2 appears after integration in two different fragments that also contain bacterial DNA from one side or the other of* $\alpha_3\beta_3$, *but fragment f4 remains unchanged. The IS3 elements flanking the F DNA in the lower part of the figure have mixed subscripts to indicate that they are recombination products. The f2A fragment is defined as the junction fragment more closely linked to proximal Hfr markers. It is present in type IA F' plasmids (32). Fragment f2B is more closely linked to distal Hfr markers and is present in type IB F' plasmids. Integration of F within f4 would leave f2 unchanged and would generate altered junction fragments f4A and f4B (not shown).*

within *Eco*RI fragment f4) the sequences of f4 would be distributed into two junction fragments (f4A and f4B), and f2 would remain unaltered. This allows localization of F integration either to *Eco*RI fragment f2 or to fragment f4. The nomenclature for junction fragments is further explained in the legend to Fig. 2.

pRH1, pRH7, pRH17, and pRH38 were digested with *Eco*RI and subjected to slab gel agarose electrophoresis (Fig. 3). Each plasmid generates approximately 50 to 60 fragments, many of which are present in all four plasmids. Because of the large number of fragments, there are several bands formed by comigrating fragments. These multiple bands were resolved in other experiments by agarose gel electrophoresis in tube gels, using low-voltage gradients (35) and extended run times.

(ii) Hybridization analysis. To identify clearly F fragments f2 and f4 and their respective bacterial junction fragments, DNA from agarose slab gels was transferred to nitrocellulose filters and was hybridized to either ^{3}H-labeled f2 or ^{3}H-labeled f4 DNA of F. Autoradiograms of these hybridized filters are shown in Fig. 4 and 5, and the results of these experiments are summarized in Table 3. There are two types of bands seen in the autoradiograms. The intense bands arise from those restriction fragments that contain substantial amounts of f2 or f4 DNA (e.g., the junction fragments), whereas the faint bands arise from fragments containing IS*2* or IS*3*, but no other sequences homologous to the probes. These faint bands are seen because of cross-hybridization. Consider the intense bands first. The hybridization patterns show clearly that when the linkage of f2 is altered (e.g., pRH7 and pRH38, Fig. 4), the mobility of f4 is unaffected and vice versa. These hybridization patterns show that the parental Hfr strains of pRH7 and pRH38 were formed by integration events at F fragment f2, whereas the Hfr parents of pRH1 and pRH17 were formed by integration within fragment f4. The same conclusions were obtained by mobility analysis alone, using high-resolution tube gels (data not shown). The f4A fragments of pRH1 and pRH17 comigrate, as do their f4B fragments. Plasmids pRH7 and pRH38 have comigrating f2A fragments. Their f2B fragments also comigrate.

Previous physical mapping studies have iden-

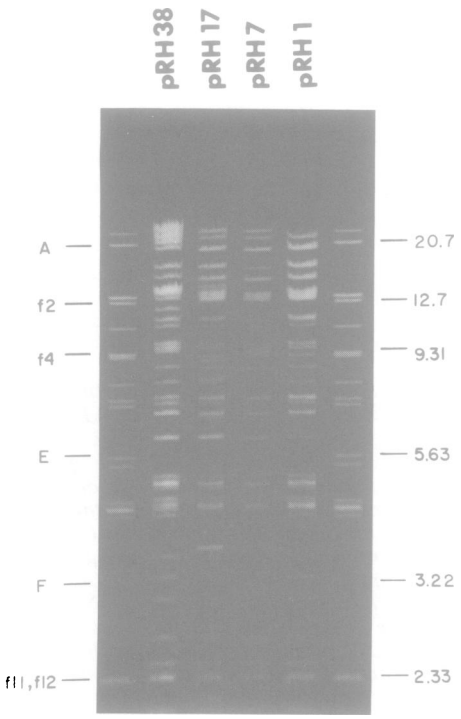

FIG. 3. *Electrophoretic analysis of EcoRI digests of pRH1, pRH7, pRH17, and pRH38. The outermost lanes contain a mixture of λ DNA and of F DNA similarly digested for use as size standards. Some of these reference bands are labeled at the left of the figure, and their sizes, in kb, are given at the right.*

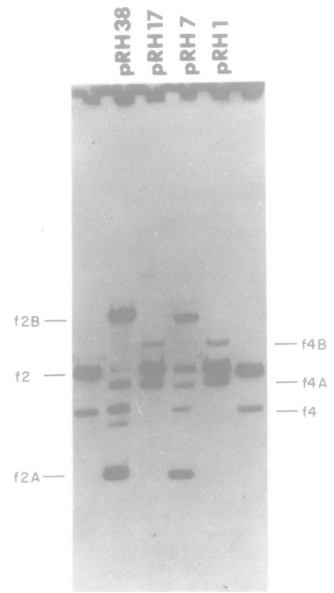

FIG. 4. *Autoradiogram of electrophoretically resolved EcoRI digests of the plasmids shown in Fig. 3, hybridized to ^{3}H-labeled f2 of F. Fragments f2, f4, and altered fragments derived from them are indicated in the figure. The lower-intensity bands represent cross-hybridization between f2 and IS3 elements present in bacterial or F DNA. Data are summarized in Table 3.*

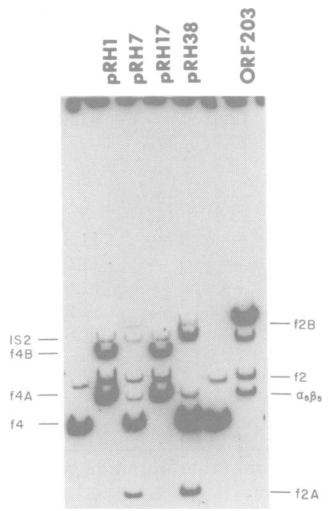

FIG. 5. *Hybridization of ^{3}H-labeled f4 to electrophoretically resolved EcoRI digests of pRH1, pRH7, pRH17, pRH38, and ORF203. In addition to f4 and fragments derived from it (areas of high intensity), the size of those EcoRI fragments containing $\alpha_5\beta_5$ and the size of f2 can be determined by comparison of hybridization patterns to the pattern of ORF203 (see Table 3). The band with highest intensity in the ORF203 pattern is its f4B. The fragment containing IS2 in all tracks is identified by its ability to hybridize with f4 but not with f2 (cf. Fig. 4). The unlabeled tracks contain a mixture of F and λ DNA. Intense hybridization to f4 of F and cross hybridization to f2 is seen in these tracks.*

tified one IS*2* element and three IS*3* elements ($\alpha_3\beta_3$, $\alpha_4\beta_4$, and $\alpha_5\beta_5$) in the region of the bacterial chromosome carried on these F′ plasmids (20, 26). Fragments visible as a result of cross-hybridization with the IS*3* contained on the f2 probe include f4 (or the f4A and f4B junction fragments), the bacterial fragment containing $\alpha_5\beta_5$ [f($\alpha_5\beta_5$)], and the fragment containing $\alpha_4\beta_4$ [f($\alpha_4\beta_4$)]. These each contain one copy of IS*3* that can cross-hybridize with the IS*3* $\alpha_1\beta_1$ on f2. With the f4 probe, the fainter cross-hybridization bands can include f2 (or f2A and f2B), f($\alpha_4\beta_5$), f($\alpha_4\beta_4$), and the bacterial restriction fragment containing IS*2*. With both probes, hybridization to $\alpha_3\beta_3$ sequences comprises part of the intense junction bands. The IS*2* element present between *lac* and *proC* is found within an 18.7-kb *Eco*RI fragment that is present in all F*lac*$^+$ *proC*$^+$ *purE*$^+$ plasmids and that hybridizes to f4 but not to f2. The 11.3-kb fragment that hybridizes to both f2 and f4 (Fig. 4 and 5) in pRH7, pRH38, and ORF203 is identified as the one containing the $\alpha_5\beta_5$ element. The bacterial IS*3* element $\alpha_4\beta_4$ can be identified within a 12.9-kb *Eco*RI fragment by its presence on pRH7 and its absence from ORF203 and from the F*lac*$^+$ *proC*$^+$ plasmid pRH96 (Table 3). This band is clearly absent from pRH38 (Fig. 5). Bands of the same sizes as those assigned to $\alpha_4\beta_4$ and to $\alpha_5\beta_5$ are also found by hybridization of f2 probe to chromosomal DNA of *E. coli* that has been digested with *Eco*RI (18).

Hybridization and mobility experiments using DNA from F42-1, pRH7, and pRH38 indicate that these plasmids have identical f2B junctions, confirming that in the parental Hfr strains of pRH7 and pRH38 (OR11 and B5), F was integrated at $\alpha_3\beta_3$ via crossover at its $\alpha_1\beta_1$ sequence (as was found for P804 [17]). The molecular length of f2B, along with the known *Eco*RI map of F (39), allows one to calculate that there should be an *Eco*RI restriction site 12.8 kb clockwise of $\alpha_3\beta_3$ on the bacterial chromosome. From the molecular length of the portion of f2 calculated to be in f2A, one can conclude that there should be a bacterial *Eco*RI restriction site 3.3 kb counterclockwise of $\alpha_3\beta_3$. This indicates that $\alpha_3\beta_3$ should be present in a 17.4-kb *Eco*RI fragment in F$^-$ *E. coli* K-12 strains. An IS*3*-carrying *Eco*RI fragment of this size has been observed in several *E. coli* K-12 strains (18). The presence of both f2A and f2B fragments, together with successful prediction of the molecular size of the bacterial fragment containing $\alpha_3\beta_3$, indicate that these plasmids are type II F′ plasmids, as will be discussed in detail below.

Because the F sequences in the Hfr progenitor strains of pRH1 and pRH17 were integrated within f4, one might hypothesize that the integrative crossover event occurred between the bacterial $\alpha_3\beta_3$ and $\alpha_2\beta_2$ of F. This hypothesis can be checked by determining whether bacterial *Eco*RI sites predicted from the F map and the molecular lengths of f4A and f4B agree with the predictions based on the f2A and f2B junction data for pRH7 and pRH38. From pRH1 and pRH17, assuming integration at $\alpha_2\beta_2$ of F, the prediction is made that the *Eco*RI site immediately counterclockwise of $\alpha_3\beta_3$ would be located 6.9 kb away, whereas the *Eco*RI site immediately clockwise would be 10.1 kb away. These values are clearly in disagreement with the values of 3.3 and 12.8 kb derived from the hybridization patterns of pRH7 and pRH38. The discrepancy is resolved by heteroduplex mapping (see below), which indicates that the integration events occurred at a new IS*3* located in f4 and not at $\alpha_2\beta_2$.

(iii) Electron microscope heteroduplex analysis. To define more precisely the junctions of the different Hfr strains and to resolve the discrepancy in predicted restriction sites immediately clockwise and counterclockwise of $\alpha_3\beta_3$, the four *tra*$^+$ plasmids, pRH1, pRH7, pRH17,

TABLE 3. *Identification and kb sizes of EcoRI fragments hybridizing to EcoRI fragments f2 or f4 of F*[a]

Plasmid	Probe	Size (kb)											
		f4B'[b]	f2B	f(IS2)	f(IS2')[c]	Joint[d]	f4B	f($\alpha_4\beta_4$)	f2	f4A	f($\alpha_3\beta_3$)	f4	f2A
ORF203	f4	25.5	—	—	—	18.8	—	—	12.8	—	11.3	—	—
pRH1	f2	—	—	—	—	—	16.4	*e*	12.8	11.7	*f*	—	—
	f4	—	—	18.9	—	—	16.2	*e*	12.8	11.3	*f*	—	—
pRH17	f2	—	—	—	—	—	16.4	*e*	12.8	11.7	*f*	—	—
	f4	—	—	19.7	—	—	16.2	*e*	12.8	11.3	*f*	—	—
pRH7	f2	—	23.5	—	—	—	—	12.8	—	—	11.3	9.4	6.0
	f4	—	24.8	19.7	—	—	—	13.3	—	—	11.5	9.5	6.2
pRH38	f2	—	25.6	—	—	—	—	—	—	—	11.6	9.4	6.1
	f4	—	23.4	19.0	20.1	—	—	—	—	—	11.3	10.3	6.1
pRH96	f4	—	24.5	19.5	—	—	—	—	—	—	11.6	9.6	—
F42-1	f4	—	23.5	—	—	—	—	—	—	—	—	9.4	—
Avg[g]		25.5 (25.0)	24.2 (24.1)	19.4 (18.7)	20.1 (19.9)	18.8 (18.4)	16.3 (16.2)	13.0 (12.9)	12.8 (12.8)	11.5 (11.4)	11.4 (11.3)	9.6 (9.3)	6.1 (6.0)

[a] Data are taken from autoradiographs shown in Fig. 4 and 5, and from other autoradiographs not shown. —, No detectable hybridization with indicated probe.

[b] Characteristic of ORF203. Values indicate the average of two measurements. The ORF203 f4A *Eco*RI fragment size is 3.0 kb and it had exited the gel for these runs; thus it does not appear (Deonier and Hadley, unpublished data).

[c] A bacterial fragment containing IS*2* and found in pRH38 but not in the other plasmids shown.

[d] The ORF203 joint *Eco*RI fragment is the fusion product resulting from recombination between $\alpha_3\beta_3$ and $\alpha_4\beta_4$ during the F' excision event.

[e] Obscured by *Eco*RI fragment f2 hybridization.

[f] Obscured by *Eco*RI fragment f4A hybridization.

[g] Values in parentheses indicate averages from mobility analysis of numerous other agarose gel electrophoresis experiments.

and pRH38, were subjected to heteroduplex analysis.

Heteroduplexes formed between FΔ(33-43) and pRH7 yielded structures expected for a type II F-prime derived from an Hfr with F integrated at its $\alpha_1\beta_1$. All of the F sequences were found to be present in pRH7 and, in incomplete heteroduplex structures, the junctions between F and the bacterial DNA were found to be at either 93.1 ± 1.8F on the F map (i.e., near the counterclockwise end of $\alpha_1\beta_1$), by measuring the shorter duplex distance from the Δ(33-43) loop to the junction with bacterial DNA, or at 94.6 ± 1.8F (i.e., near the clockwise end of $\alpha_1\beta_1$), by measuring the longer distance. There were no insertions or substitutions within the F sequences of pRH7.

The structure of pRH38 was verified by forming heteroduplexes between it and F42-1, a derivative of the classical F*lac*. Because the Hfr from which pRH38 arose was derived from W1655F$^+$, a deletion from 32.6F to 42.3F was expected, and such a deletion was found. Structures were detected that indicated complete homology between F42-1 and pRH38 in the vicinity of the junction between F-sequences near $\alpha_1\beta_1$ and the bacterial DNA counterclockwise of *lac*, verifying that one junction of pRH38 includes $\alpha_1\beta_1$. Since F sequences from 0.0F to 2.8F are deleted in F42-1, this set of heteroduplexes did not directly prove the presence of these sequences in pRH38. Their presence is inferred from the hybridization data, however, which support the electron microscope data indicating that pRH38 is a type II F'. An unexpected feature seen with pRH38/F42-1 heteroduplexes was an insertion of 1.4 ± 0.3 kb located at 55.3F, within *Eco*RI fragment f3. This alteration produced a band with a molecular length of 12.3 kb, which was detected electrophoretically as well. The altered f3 band did not hybridize to IS*2* or IS*3* (Fig. 5, Table 3).

The pRH1/FΔ(33-43) heteroduplex experiments yielded also two unexpected structure types composed in part of incomplete pRH1 strands, and the interpretations of these structures are summarized in Fig. 6. Instead of displaying uninterrupted duplex between the fork at the F/bacterial junction and the Δ(33-43) deletion loop, these structures possessed additional deletion loops. The larger single-strand loop (Fig. 6B), which defines one structure type, was 21 kb from the Δ(33-43) loop and was separated from the single-strand fork by a duplex region 1.2 kb in length. The loop size was 12.2 ± 0.8 kb (single-strand measurement). The other structure type contained a smaller single-strand loop, whose size is 2 kb. This loop was located approximately 63 to 64 kb from the Δ(33-43)

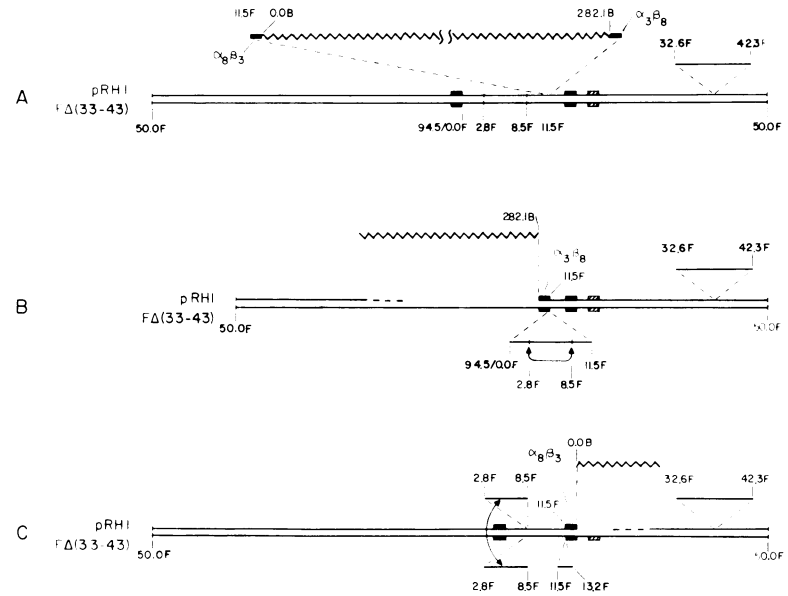

FIG. 6. *Diagrams of observed pRH1/FΔ(33-43) heteroduplex structures. The circular F portions of the structure have been arbitrarily drawn in a linear fashion for clarity. Bacterial DNA, F DNA, and IS elements are indicated as in Fig. 1. A complete heteroduplex structure is depicted in panel A. All of the F DNA is present in pRH1, and there was a large single-strand insertion loop at the indicated position. Panels B and C depict the structures that led to the interpretation that the Hfr parent of pRH1 was the result of recombination between $\alpha_3\beta_3$ and a new IS3 ($\alpha_8\beta_8$) on F. For the structure in panel B, pRH1 DNA extending counterclockwise from 11.5F to some point beyond $\alpha_1\beta_1$ is missing because of strand breakage. The 1.3-kb duplex near 282.1B is seen to be the result of hybridization of $\alpha_3\beta_8$ to $\alpha_1\beta_1$ on the F strand. The deletion loop at 11.5F contains inverted repetitions at 2.8F and 8.5F, and these can hybridize (indicated by arrows) to form the interior loop seen in all cases. In panel C, pRH1 DNA extending clockwise of 11.5F is missing. Thus, $\alpha_8\beta_3$ can hybridize to $\alpha_2\beta_2$ to form a 1.3-kb duplex flanked by the 11.5F-13.2F loop and a fork. The 2.8F-8.5F portions of both FΔ(33-43) and pRH1 are drawn as insertion-deletion loops. If they hybridize in the configuration shown (stabilized by the short inverted repetitions at 2.8F and 8.5F), a characteristic loop (9) can form. This feature was seen.*

deletion loop, and it was separated from a single-strand fork by a duplex region of length 1.3 kb. The interpretations appearing in Fig. 6 are based on these observations and on other structures described in the figure legend. Both of these types of structures can be rationalized by assuming that the junctions between F and the bacterial DNA in pRH1 occur at 11.5 on the F map, with IS*3* elements separating F from the bacterial DNA at each junction. This is the structure that would be expected if the F plasmid which mediated the F integration event leading to the Hfr parent of pRH1 contained an additional IS*3* at 11.5F. The F plasmid of the F^+ K-12-112 derivative which led to the Hfr parents of pRH1 and pRH17 does contain an additional IS*3* located in f4 (Hadley and Deonier, unpublished data). We call this IS*3* $\alpha_8\beta_8$, and the two product IS*3* elements arising from recombination between it and $\alpha_3\beta_3$ are called $\alpha_8\beta_3$ or $\alpha_3\beta_8$. Heteroduplex structures formed from pRH17 (also derived from a K-12-112 F^+) and FΔ(33-43) also indicated that the integration site on F was 11.5F, and structures similar to those depicted in Fig. 6C were seen. Because of strand breakage, structures like the one shown in Fig. 6B were not seen during the limited examination of this plasmid DNA.

By using the heteroduplex data, which indicate a junction between F and bacterial sequences at 11.5F, one can now employ the molecular lengths for the fragments f4A and f4B obtained electrophoretically to fix the positions on the bacterial DNA of the restriction sites immediately clockwise and immediately counterclockwise of $\alpha_3\beta_3$. The values obtained, 12.3 and 3.4 kb, agree reasonably well with the values calculated from pRH7 and pRH38 electrophoretic data. The presence of both f4A and f4B fragments whose sizes provide consistent mapping of the *Eco*RI cleavage sites immediately clockwise and counterclockwise of $\alpha_3\beta_3$ indicates that pRH1 and pRH17, like pRH7 and pRH38, are type II F′ plasmids.

Analysis of bacterial sequences present on pRH plasmids. As discussed earlier, the

presence of a complete complement of F sequences and the presence of f2A and f2B (or f4A and f4B) junction fragments indicate that pRH1, pRH7, pRH17, and pRH38 are type II F′ plasmids. Confirmation of this is provided by analysis of the bacterial restriction fragments carried by them and by certain reference plasmids. Table 4 shows some of the fragments resulting from *Eco*RI digestion of various plasmids. Only the fragments located counterclockwise of $\alpha_3\beta_3$ and in the region extending from $\alpha_3\beta_3$ to *lac* are shown here. Fragments present on both pRH111 (a *tra*Δ*F proA*$^+$ to be described elsewhere) and F128, but missing from ORF203, define the group located counterclockwise of $\alpha_3\beta_3$. Fragments present on both F128 and F42-1 define the group of fragments extending clockwise of $\alpha_3\beta_3$ to just beyond *lac*. It is seen that pRH1, pRH7, pRH17, pRH38, and pRH97 all contain restriction fragments characteristic of the *lac* region and that they also contain restriction fragments counterclockwise of the integration site. The presence of restriction fragments from both sides of the F integration site again indicates that these F′ plasmids are type II.

The pRH96 is an exception; it lacks bacterial DNA common to both pRH111 and F128 and thus is missing bacterial DNA counterclockwise of $\alpha_3\beta_3$. Moreover, one of the F fragments (f11 or f12, which usually migrate together) is missing. Fragment f11 is located between 25F and 28F on the F map, and other F′ plasmids from the same Hfr parent show no alteration in this region of F sequences. If pRH96 were to have excised at 2.8 on the F map, which is one end of the translocatable γδ element, fragment f12 would be altered in its linkage to other F fragments and would no longer appear. This suggests that pRH96 is a type I F′ which may have excised at 2.8F, a known hot spot for F′ excision. This interpretation is supported by the absence of the 6.08-kb f2A junction fragment. This fragment is characteristic of all of the type II F′ plasmids arising from Hfr strains that resulted from integration of F via its $\alpha_1\beta_1$ IS*3* element at $\alpha_3\beta_3$, and it was seen in pRH7, pRH38, pRH95, pRH97, and pRH98.

Specificity of the F′ plasmid excision process. As seen in Table 2, pRH1, pRH7, pRH95, pRH97, and pRH98 have almost identical molecular sizes. It is also seen from Fig. 7, Fig. 8, and Table 4 that these plasmids are identical within the resolution of the present restriction enzyme analysis (except for the differences in linkage of F sequences to bacterial sequences in pRH1). Plasmids pRH7, pRH95, pRH97, and pRH98 were derived from an Hfr strain in which F had integrated within $\alpha_1\beta_1$, whereas pRH1 was derived from an Hfr in which F had integrated at the new IS*3* element located at 11.5F on the F map ($\alpha_8\beta_8$). Plasmids pRH7, pRH95, pRH97, and pRH98 gave identical restriction patterns regardless of whether they were digested with *Eco*RI or with *Bam*HI (Fig. 7 and 8). We emphasize that these F′ plasmids are independent of each other in the sense that they were isolated from Hfr cultures that were started from different single colonies derived from OR11. Plasmid pRH1 was derived from OR6, an independent Hfr strain. Because the bacterial DNA present on plasmids pRH1, pRH7, pRH95, pRH97, and pRH98 is identical within experimental error, then both of the excisional loci for these five plasmids are the same, unless they differ by being shifted exactly the same distance either clockwise or counterclockwise within the distance spanned by one *Eco*RI fragment. We prefer the former explanation. The conclusion is that type II excision can be a precise, repeatable event.

The excision loci for pRH1, pRH7, pRH95, pRH97, and pRH98 can be determined both from the presence of characteristic *Eco*RI restriction fragments mapped in the *proA* to *purE* region of the bacterial chromosome, and by comparison with the *Eco*RI restriction pattern of F13. In Table 4 are indicated some of the *Eco*RI restriction fragments between *proA* and $\alpha_3\beta_3$. The 6.8-kb, 4.6-kb, 4.5-kb and 3.6-kb fragments shared by pRH1, pRH7, and pRH97 comprise a cluster that is located immediately counterclockwise of f($\alpha_3\beta_3$), the bacterial *Eco*RI fragment containing $\alpha_3\beta_3$. The first fragment counterclockwise of this cluster has a size of 14.9 kb (R. G. Hadley and R. C. Deonier, manuscript in preparation). The 14.9-kb fragment and all other fragments counterclockwise of it are missing from these plasmids, whereas all resolved fragments clockwise of the 14.9-kb fragment are present. Thus one of the recombination sites active in F′ excision lies within the 14.9-kb fragment (Fig. 1). A similar argument based on which *Eco*RI fragments are present may be used to locate the clockwise recombination regions for these five plasmids; they all lie within the first *Eco*RI fragment clockwise of f($\alpha_4\beta_4$) (see legend to Fig. 1). These assignments are confirmed and refined when the restriction patterns for these plasmids are compared with the pattern for F13. Except for alterations associated with the different linkages of F and the bacterial DNA (Fig. 1, Table 5) and alteration of a bacterial fragment also noted in pRH38 (which, like F13, is derived from the W6F$^+$ subline), the *Eco*RI restriction patterns for F13 and the five plasmids pRH1, pRH7, pRH95, pRH97, and pRH98 are identical. This strongly suggests that the excision sites for all of these plasmids are

TABLE 4. *Fragments generated by restriction endonuclease EcoRI from F' plasmids carrying various portions of the proA-lac region of the E. coli K-12 chromosome*[a]

Region of chromosome	Fragment size (kb) generated from the following plasmid:									
	pRH1	pRH7	pRH97	pRH38	pRH17	ORF203	F128	F42-1	pRH111	pRH96
proA to $\alpha_3\beta_3$	—[b]	—	—	—	—	—	15.07	—	14.87	—
	—	—	—	—	—	—	—	—	14.03	—
	—	—	—	—	—	—	10.18	—	10.17	—
	6.86	6.82	6.91	6.82	6.80	—	6.84	—	6.79	—
	—	—	—	—	—	—	5.76	—	5.74	—
	—	—	—	—	—	—	5.60	—	5.57	—
	4.62	4.61	4.68	4.62	4.57	—	4.56	—	4.62	—
	4.54	4.48	4.50	4.50	4.43	—	4.42	—	4.48	—
	3.61	3.61	3.66	3.62	3.62	—	3.65	—	3.63	—
	—	—	—	—	—	—	—	—	1.74	—
	—	—	—	—	—	—	—	—	1.62	—
	—	—	—	—	—	—	—	—	1.48	—
	*[c]	0.50	*	0.50	*	—	0.52	—	0.50	—
$\alpha_3\beta_3$ to *lac*	21.62	21.56	21.65	21.25	21.37	21.74	21.23	21.68	—	21.82
	4.93	4.92	5.15	4.92	4.90	4.93	4.96	4.94	—	4.99
	2.68	2.68	2.63	2.69	2.68	2.71	2.69	2.72	—	2.68
	2.47	2.47	2.41	2.47	2.46	2.48	2.43	2.50	—	2.47
Novel joints and identification	16.16(f4B)	23.92(f2B)	23.90(f2B)	23.59(f2B)	16.16(f4B)	25.0(f4B)	24.44(f2B)	24.11(f2B)	11.47(f4A)	23.87(f4B)
	14.83(J)[d]	14.92(J)	15.20(J)	13.32(J)		18.40(J)	21.79(J)	9.60(f12A)	3.27(f6J)	8.02(f12J)
	11.42(f4A)	6.05(f2A)	6.15(f2A)	6.05(f2A)	11.40(f4A)	2.98(f4A)	6.08(f2A)			

[a] For simplicity, those fragments containing F DNA only, or bacterial DNA extending clockwise from *lac* to $\alpha_4\beta_4$ and beyond, have been omitted from this tabulation. Standard deviations are ±0.2 kb for 20-kb fragments, ±0.04 kb for 10-kb fragments, and ±0.06 kb for 5-kb fragments. The additional digit has been retained to indicate that closely migrating bands could be discriminated on individual gels.

[b] —, Absent from the plasmid.

[c] *, Not resolved.

[d] Novel joint fragments (J) are those modified restriction fragments generated during F' formation.

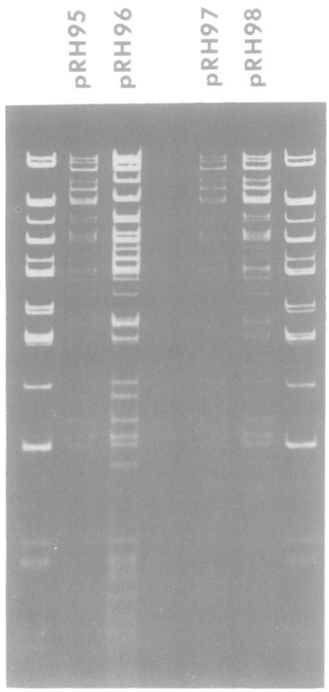

FIG. 7. *Electrophoretic analysis of pRH95, pRH96, pRH97, and pRH98 after digestion with EcoRI. The outer tracks contain a mixture of λ DNA and F DNA digested with EcoRI. Except for pRH96, the other pRH plasmids displayed band patterns that were identical to the pattern for pRH7 (Fig. 3).*

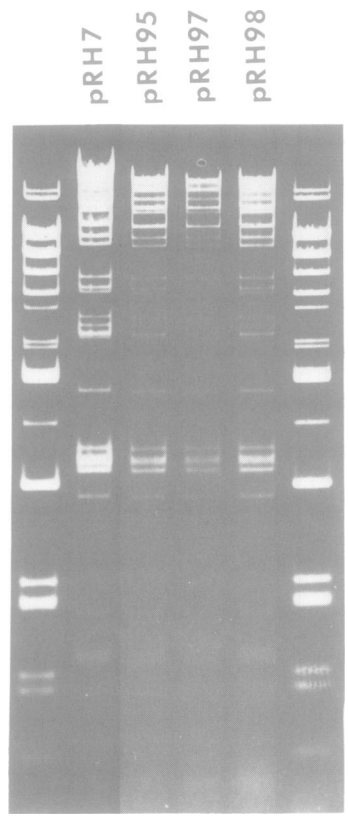

FIG. 8. *Electrophoretic analysis of pRH7, pRH95, pRH97, and pRH98 after digestion with BamHI. The outer tracks contain mixtures of λ DNA and FΔ(33–43) DNA digested with EcoRI. The photographic negative was scanned with a microdensitometer for quantitative analysis. The positions of the bands generated from the four plasmids shown were superimposable, and the relative peak intensities in each track were all the same.*

identical to those of F13. The length measurements from heteroduplex data (26) indicate that the F13 termini lie in just those restriction fragments to which the termini of pRH1, pRH7, pRH95, pRH97, and pRH98 are assigned from restriction fragment mapping data.

Similar analysis of *Eco*RI fragments present in pRH17 indicates that its counterclockwise excision endpoint also lies in the 14.9-kb *Eco*RI fragment between *proA* and $\alpha_3\beta_3$. However, its clockwise excision endpoint lies approximately 100 kb clockwise of $\alpha_4\beta_4$, in contrast to the other plasmids discussed here. The clockwise excision point of pRH38 also clearly differs from those of the other plasmids. Plasmid pRH38 does not contain $\alpha_4\beta_4$ (Table 3). The *Eco*RI fragment immediately counterclockwise of f($\alpha_4\beta_4$) has a size of either 9.5 or 14.8 kb. These two fragments are adjacent, but their order has not yet been determined. Because pRH38 does contain the 9.5-kb *Eco*RI fragment, it is possible to deduce a maximum span within which the clockwise endpoint of pRH38 is located. The clockwise excision point is located within an interval no larger than 19 kb [14.8 kb + the distance from $\alpha_4\beta_4$ to the counterclockwise restriction site defining f($\alpha_4\beta_4$)]. The length of bacterial DNA carried by pRH38 (272 kb) allows mapping of the counterclockwise excision point of this plasmid within an interval between 32 and 51 kb counterclockwise of $\alpha_3\beta_3$. This overlaps the region containing the counterclockwise excision termini of all of the other type II F′ plasmids described here, suggesting that all seven of the type II pRH plasmids and F13 share a common counterclockwise excision site.

DISCUSSION

The results obtained in this study clarify and extend current concepts concerning the process of F′ formation. First, contrary to previous indications (32), the type II excision process (43) appears to be more frequent than the type I process, at least in this region of the bacterial

TABLE 5. *Comparison of differences in EcoRI fragments generated from pRH7 and F13*[a]

Fragment size (kb)	Presence in plasmid		Identification[b]
	F13	pRH7	
25.0	+	−	F13 f4B junction[c]
23.9	−	+	pRH7 f2B junction
20.2	+	−	F13 bacterial fragment with IS*2* insertion[d]
18.9	−	+	Bacterial fragment altered above in F13[d]
18.9	−	+	Normal f(IS*2*)
17.2	+	−	Normal f($\alpha_3\beta_3$)
12.7	+	−	Normal f2 of F
9.31	−	+	Normal f4 of F
6.05	−	+	pRH7 f2A junction
2.98	+	−	F13 f4A junction[c]

[a] Except for the fragments listed, the patterns for the two plasmids are identical.

[b] See Fig. 1. All predicted differences between pRH7 and F13 are visible.

[c] The f4B and f4A junction fragments of F13 are identical to those of ORF203 (see Table 4).

[d] Plasmid pRH38, like F13, is a derivative of the W6F$^+$ subline of *E. coli* K-12. It shows the same alteration seen with F13, and this alteration is attributed to an IS*2* insertion in an 18.9-kb bacterial fragment (see Table 3). The 18.9-kb bacterial fragment does not appear in either of the two termination regions (Hadley and Deonier, unpublished data).

chromosome. Only one of eight F′ plasmids carrying *lac* obtained in this series of experiments appeared to be type I. Plasmids like the type I F42 plasmid (the classical F*lac*) were not obtained. The apparent abundance of type I plasmids seen in earlier experiments may be explained in part either by a greater tendency for the smaller plasmids to be mobilized, or perhaps by their more efficient retention than larger type II plasmids (K. B. Low, personal communication). Thus type I F′ plasmids might be isolated at high frequencies under certain experimental conditions, regardless of whether they are primary excision products or are deletion mutants of larger, possibly type II precursors. As Low clearly indicates (32), plasmids that appear to be type I by genetic criteria may in fact be type II when exact termini are determined. Hence, even though all of the plasmids described in this work genetically appear to be type I F′ plasmids carrying markers clockwise of the F integration site (i.e., toward *lac*), all but one of them actually contains between 23 and 38 kb of bacterial DNA counterclockwise of the integrated F as well (i.e., DNA from $\alpha_3\beta_3$ to a point within the 14.9-kb fragment near *proA*).

Second, we find that in at least six, and possibly all seven cases, the counterclockwise recombination region for type II F′ excision falls within the same *Eco*RI restriction fragment, and possibly corresponds to the counterclockwise excision point of F13. However, the clockwise endpoint may either be the same (as is apparently true for pRH1, pRH7, pRH95, pRH97, pRH98, and F13) or may vary (e.g., pRH17 and pRH38 compared with the previous set). It would appear then that type II F′ excision can be either single-site specific or double-site specific (14, 33). Our experiments locate the recombination sites for excision with a precision equal to the size of one *Eco*RI restriction fragment, but comparison with F13 suggests that these sites may be identical to those active in excision of F13.

The nature of these sites is not known. One possible element that might appear at the counterclockwise site is IS*1*. It is known that IS*1* can cause deletions of neighboring DNA in which the deletion endpoint terminating at IS*1* is fixed and the other endpoint is variable (41). The observed F′ plasmids could then result from a segment of the bacterial chromosome which is deleted, but is retained in this case as a plasmid because of the presence of the F replicator. If such a mechanism were operating, however, one would expect on the basis of previous data that a much larger variety of clockwise deletion endpoints leading to a corresponding variety of plasmid sizes would be observed. Another possibility to explain excision of plasmids like pRH7 would be the presence of directly repeated sequences (like IS*1*) which are capable of causing excision or deletion of defined DNA segments. Examples of deletions mediated by direct repetitions of IS*1* are loss of the chloramphenicol transposon Tn*9* (34) and loss of the drug resistance determinants of certain fi$^+$ R plasmids (27, 40). Recombination between directly repeated IS*3* elements has been observed in formation of ORF203 (type II) (20) and F80 (type I) (38). We can exclude the possibility that recombination between direct repetitions of IS*2* or IS*3* elements is responsible for formation of these F*lac*$^+$ *proC*$^+$ *purE*$^+$ plasmids, because the novel joint fragments generated by such a mechanism would contain IS*2* or IS*3*, contrary to what was observed. Specifically, plasmids produced by this mechanism operating at $\alpha_3\beta_1$ (or $\alpha_2\beta_2$) and $\alpha_4\beta_4$ were not detected in this study. A third possibility is that *att*^{P22} is somehow involved. The counterclockwise excision points for these F′ plasmids are close to the position on the *E. coli* chromosome at which the temperate *Salmonella* bacteriophage P22 has been shown to integrate (25). It may be that this locus for site-specific bacteriophage integration, if present on the *E. coli* chromosome, can act in other site-specific recombinational processes as well. We note in this context the similarity in nucleotide sequence between *att*$^{\lambda}$ and portions

of IS*1* (29).

The tendency for high specificity in type II F′ excision, at least in the region of the bacterial chromosome studied here, is indicated by the presence of one distinguishable recombination region 23 to 38 kb counterclockwise of $\alpha_3\beta_3$ and only three other regions within a 350-kb span clockwise of $\alpha_3\beta_3$, with one of these three being used in five separate excision events. The nearest site is some 272 kb from the counterclockwise excision region. In contrast, when the type I plasmids F2 (17), F42-1 (26), and pRH96 are compared, the clockwise excision points are seen to lie 32, 53, and 206 kb clockwise of $\alpha_3\beta_3$, respectively. Similar variations were seen with the excision of F100 and F152 (37).

The significance of specific type II F′ types may be twofold. First, this could mean that F can act repeatedly as a "cloning vehicle" for specific portions of the bacterial chromosome. Because F is capable of conjugal transfer to other bacterial genera, this could mean that discrete portions of the *E. coli* chromosome are repeatedly and naturally "cloned" in vivo. The second possible area of significance derives in part from the first: if specific portions of the bacterial chromosome can be excised and mobilized, it may be that bacterial evolution can proceed by accretion of blocks of DNA, in a manner similar to the suggestion by Susskind and Botstein for lambdoid bacteriophages (46).

In addition to providing information relating to specificity in the excision of *tra*$^+$ F′ plasmids, these data allow one to determine the sizes of the *Eco*RI restriction endonuclease fragments containing previously defined bacterial IS elements and also allow the determination of additions or deletions of such elements within the bacterial segments carried by the F′ plasmids. Of the previously mapped IS elements, $\alpha_3\beta_3$ has been localized on an *Eco*RI fragment of 17.2 kb, $\alpha_4\beta_4$ is found on a fragment of 12.9 kb, $\alpha_5\beta_5$ resides on an 11.3-kb fragment, and the IS*2* element positioned near $\alpha_5\beta_5$ is found on an *Eco*RI fragment of 18.7 kb. These assignments are presented in Table 3. Plasmid pRH38 lacked $\alpha_4\beta_4$, presumably as a consequence of its being left behind on the bacterial DNA after the excision process. There is no evidence in any case for the presence of additional IS*3* elements within the bacterial sequences carried on pRH1, pRH7, pRH17, or pRH38. Hybridization did indicate the presence of an additional IS*2* within bacterial DNA of pRH38, however (Table 3). These studies have documented the presence of an unexpected IS*3* element in the F DNA of two of the F′ plasmids. Structures of F′ plasmids derived from K-12-112 background indicated that the F$^+$ plasmid in that strain possessed an IS*3* inserted at 11.5F in the same orientation as $\alpha_1\beta_1$ and $\alpha_2\beta_2$. It is interesting to note that this "new" IS*3* was involved in the integration events of both of the Hfr strains derived from the K-12-112 background documented in these studies. Heteroduplexes involving pRH38 revealed the presence of an insertion or deletion of 1.4 kb at approximately 55F. Since the *Eco*RI fragment containing this alteration does not hybridize with either f2 or f4, it does not represent an IS*2* or IS*3* insertion.

Finally, we note that the linkages between the F sequences and bacterial sequences in these F′ plasmids (which, since they are type II, are probably identical to the linkages in the parental Hfr), agree with previous predictions (14). First, there are direct repetitions of IS*3* elements at each junction of bacterial and F sequences. Second, independent Hfr strains that formed by integration events involving the same IS element of F and located at this chromosomal site produce identical junction fragments after restriction endonuclease digestion of type II F′ DNA (Table 3). Finally, type II F′ plasmids from independent Hfr strains formed by integration events at $\alpha_3\beta_3$ and employing different sequences of F produced junction fragments after restriction endonuclease digestion that carried identical bacterial sequences. This brings to six the number of F integration events at $\alpha_3\beta_3$ that have been probed by physical methods (the other two Hfr strains are P4X and P804 [17]), and the structural features shared in all six cases indicate that in this region of the *E. coli* chromosome, integration at a preexisting IS*3* element is the primary mechanism for Hfr formation.

ACKNOWLEDGMENTS

We thank Roy Curtiss III and P. M. A. Broda for generously supplying us with their strains, B. Bachmann for extensive pedigree data, and Mark Guyer and A. J. Clark for helpful comments and criticisms. This work benefited from the technical assistance of Karin Fouts and Marilyn Medieros.

Financial support for the work was provided by National Science Foundation grant no. BMS7520512 and by Public Health Service grant no. GM-24589-01 from the National Institutes of Health.

LITERATURE CITED

1. **Achtman, M., R. A. Skurray, R. Thompson, R. Helmuth, S. Hall, L. Beutin, and A. J. Clark.** 1978. Assignment of *tra* cistrons to *Eco*RI fragments of F sex factor DNA. J. Bacteriol. **133**:1383–1392.
2. **Anthony, W. M., R. C. Deonier, H.-J. Lee, S. Hu, E. Ohtsubo, and N. Davidson.** 1974. Electron microscope heteroduplex studies of sequence relations among plasmids of *Escherichia coli*. IX. Note on the deletion mutant of F, FΔ(33–43). J. Mol. Biol. **89**:647–650.
3. **Bazaral, M., and D. R. Helinski.** 1972. Circular DNA forms of colicinogenic factors E1, E2, and E3 from *Escherichia coli*. J. Mol. Biol. **36**:185–194.
4. **Berg, C. M., and R. Curtiss III.** 1967. Transposition derivatives of an Hfr strain of *Escherichia coli* K-12. Genetics **56**:503–525.

5. **Botchan, M., W. Topp, and J. Sambrook.** 1976. The arrangement of simian virus 40 sequences in the DNA of transformed cells. Cell **9**:269-287.
6. **Broda, P.** 1967. The formation of Hfr strains in *Escherichia coli* K12. Genet. Res. **9**:34-47.
7. **Broda, P., J. R. Beckwith, and J. Scaife.** 1964. The characterization of a new type of F-prime in *Escherichia coli* K-12. Genet. Res. **5**:489-494.
8. **Broda, P., and P. Meacock.** 1971. Isolation and characterization of Hfr strains from a recombination deficient strain of *Escherichia coli*. Mol. Gen. Genet. **113**:166-173.
9. **Broker, T. R., L. T. Chow, and L. Soll.** 1977. The *E. coli* gamma-delta recombination sequence is flanked by inverted duplications, p. 575-580. *In* A. I. Bukhari, J. A. Shapiro, and S. L. Adhya (ed.), DNA insertion elements, plasmids, and episomes. Cold Spring Harbor Laboratory, Cold Spring Harbor, N.Y.
10. **Childs, G. J., H. Ohtsubo, E. Ohtsubo, F. Sonnenberg, and M. Freundlich.** 1977. Restriction endonuclease mapping of the *Escherichia coli* K12 chromosome in the vicinity of the *ilv* genes. J. Mol. Biol. **117**:175-193.
11. **Clarke, L., and J. Carbon.** 1976. A colony bank containing synthetic ColE1 hybrid plasmids representative of the entire *E. coli* genome. Cell **9**:91-99.
12. **Clowes, R. C., and W. Hayes (ed.).** 1968. Experiments in molecular genetics. John Wiley & Sons, Inc., New York.
13. **Curtiss, R., III, and D. R. Stallions.** 1969. Probability of F integration and frequency of stable Hfr donors in F' populations of *Escherichia coli* K-12. Genetics **63**: 27-38.
14. **Davidson, N., R. C. Deonier, S. Hu, and E. Ohtsubo.** 1975. Electron microscope heteroduplex studies of sequence relations among plasmids of *Eschericha coli*. X. Deoxyribonucleic acid sequence organization of F and F-primes and the sequences involved in Hfr formation, p. 56-65. *In* D. Schlessinger (ed.), Microbiology—1974. American Society for Microbiology, Washington, D.C.
15. **Davis, R., W. M. N. Simon, and N. Davidson.** 1971. Electron microscope heteroduplex methods for mapping regions of base sequence homology in nucleic acids. Methods Enzymol. **21**:413-428.
16. **Denhardt, D. T.** 1966. A membrane-filter technique for the detection of complementary DNA. Biochem. Biophys. Res. Commun. **23**:641-646.
17. **Deonier, R. C., and N. Davidson.** 1976. The sequence organization of the integrated F plasmid in two Hfr strains of *Escherichia coli*. J. Mol. Biol. **107**:207-222.
18. **Deonier, R. C., R. G. Hadley, and M. Hu.** 1979. Enumeration and identification of IS3 elements in *Escherichia coli* strains. J. Bacteriol. **137**:1421-1424.
19. **Deonier, R. C., and L. Mirels.** 1977. Excision of F plasmid sequences by recombination at directly repeated insertion sequence 2 elements: involvement of *recA*. Proc. Natl. Acad. Sci. U.S.A. **74**:3965-3969.
20. **Deonier, R. C., G. R. Oh, and M. Hu.** 1977. Further mapping of IS2 and IS3 in the *lac-purE* region of the *Escherichia coli* K-12 genome: structure of the F-prime ORF203. J. Bacteriol. **129**:1129-1140.
21. **De Witt, S. K., and E. A. Adelberg.** 1962. The occurrence of a genetic transposition in a strain of *Escherichia coli*. Genetics **47**:577-585.
22. **Engel, J. D., and J. B. Dodgson.** 1978. Analysis of adult and embryonic chicken globin genes in chromosomal DNA. J. Biol. Chem. **254**:8239-8246.
23. **Hirota, Y., and P. H. A. Sneeth.** 1961. F-prime and F mediated transduction in *Escherichia coli* K-12. Jpn. J. Genet. **36**:307-318.
24. **Hoppe, I., and J. Roth.** 1974. Specialized transducing phages derived from Salmonella phage P22. Genetics **76**:633-654.
25. **Howard-Flanders, P., and L. Theriot.** 1966. Mutants of *Escherichia coli* defective in DNA repair and in genetic recombination. Genetics **53**:1137-1150.
26. **Hu, S., E. Ohtsubo, and N. Davidson.** 1975. Electron microscope heteroduplex studies of sequence relations among plasmids of *Escherichia coli*: structure of F13 and related F-primes. J. Bacteriol. **122**:749-763.
27. **Hu, S., E. Ohtsubo, N. Davidson, and H. Saedler.** 1975. Electron microscope heteroduplex studies of sequence relations among bacterial plasmids: identification and mapping of the insertion sequences IS1 and IS2 in F and R plasmids. J. Bacteriol. **122**:764-775.
28. **Jacob, F., A. Ullman, and J. Monod.** 1965. Délétions fusionnant l'opéron lactose et un opéron purine chez *Escherichia coli*. J. Mol. Biol. **31**:704-719.
29. **Landy, A., and W. Ross.** 1977. Viral integration and excision: structure of the lambda *att* sites. Science **197**: 1147-1160.
30. **Laskey, R. A., and A. D. Mills.** 1975. Quantitative film detection of ^{3}H and ^{14}C in polyacrylamide gels by fluorography. Eur. J. Biochem. **56**:335-341.
31. **Lennox, E. S.** 1955. Transduction of linked genetic characters of the host by bacteriophage P1. Virology **1**:190-260.
32. **Low, K. B.** 1972. *Escherichia coli* K-12 F-prime factors, old and new. Bacteriol. Rev. **36**:587-607.
33. **Low, K. B., and R. D. Porter.** 1978. Modes of gene transfer and recombination in bacteria. Annu. Rev. Genet. **12**:249-287.
34. **MacHattie, L. A., and J. B. Jackowski.** 1977. Physical structure and deletion effects of the chloramphenicol resistance element Tn9 in phage lambda, p. 219-228. *In* A. I. Bukhari, J. A. Shapiro, and S. L. Adhya (ed.), DNA insertion elements, plasmids, and episomes. Cold Spring Harbor Laboratory, Cold Spring Harbor, N.Y.
35. **McDonell, M. W., M. N. Simon, and F. W. Studier.** 1977. Analysis of restriction fragments of T7 DNA and determination of molecular weights by electrophoresis in neutral and alkaline gels. J. Mol. Biol. **110**:119-146.
36. **Morrow, J. F., S. N. Cohen, A. C. Y. Chang, H. W. Boyer, M. H. Goodman, and R. B. Helling.** 1974. Replication and transcription of eucaryote DNA in *Escherichia coli*. Proc. Natl. Acad. Sci. U.S.A. **71**:1743-1747.
37. **Ohtsubo, E., and M.-T. Hsu.** 1978. Electron microscope heteroduplex studies of sequence relations among plasmids of *Escherichia coli*: structure of F100, F152, and F8 and mapping of the *Escherichia coli* chromosomal region *fep-supE-gal-attλ-uvrB*. J. Bacteriol. **134**:778-794.
38. **Ohtsubo, E., and M. T. Hsu.** 1978. Electron microscope heteroduplex studies of sequence relations among plasmids of *Escherichia coli*: isolation of a new F-prime factor, F80, and its implication for the mechanism of F integration into the chromosome. J. Bacteriol. **134**:795-800.
39. **Ohtsubo, H., and E. Ohtsubo.** 1977. Repeated DNA sequences in plasmids, phages, and bacterial chromosomes, p. 49-64. *In* A. Bukhari, J. Shapiro, and S. Adhya (ed.), DNA insertion elements, plasmids, and episomes. Cold Spring Harbor Laboratory, Cold Spring Harbor, N.Y.
40. **Ptashne, K., and S. N. Cohen.** 1975. Occurrence of insertion sequence regions on plasmid deoxyribonucleic acid as direct and inverted nucleotide sequence duplications. J. Bacteriol. **122**:776-781.
41. **Reif, H. J., and H. Saedler.** 1975. IS1 is involved in deletion formation in the *gal* region of *E. coli* K-12. Mol. Gen. Genet. **137**:17-28.
42. **Rigby, P. W., M. Dieckmann, C. Rhodes, and P. Berg.** 1977. Labeling deoxyribonucleic acid to high specific activity *in vitro* by nick translation with DNA polymerase I. J. Mol. Biol. **113**:237-251.
43. **Scaife, J.** 1967. Episomes. Annu. Rev. Microbiol. **21**:601-

638.

44. **Sharp, P. A., M.-T. Hsu, E. Ohtsubo, and N. Davidson.** 1972. Electron microscope heteroduplex studies of sequence relations among plasmids of *Escherichia coli*. J. Mol. Biol. **71**:471-497.
45. **Southern, E. M.** 1975. Detection of specific sequences among DNA fragments separated by gel electrophoresis. J. Mol. Biol. **98**:503-517.
46. **Susskind, M. M., and D. Botstein.** 1978. Molecular genetics of bacteriophage P22. Microbiol. Rev. **42**:385-413.
47. **Thomas, M., and R. W. Davis.** 1975. Studies on cleavage of bacteriophage lambda DNA with *Eco*RI restriction endonuclease. J. Mol. Biol. **91**:315-328.
48. **Thompson, R., S. G. Hughes, and P. Broda.** 1974. Plasmid identification using specific endonucleases. Mol. Gen. Genet. **133**:141-149.